UNIVERSITÄT AUGSBURG
Universitätsbibliothek

OPEN ACCESS
OPUS AUGSBURG

Geometric properties of integrable Kepler and Hooke billiards with conic section boundaries

Daniel Jaud, Lei Zhao

Angaben zur Veröffentlichung / Publication details:

Jaud, Daniel, and Lei Zhao. 2024. "Geometric properties of integrable Kepler and Hooke billiards with conic section boundaries." *Journal of Geometry and Physics* 204: 105289. https://doi.org/10.1016/j.geomphys.2024.105289.

Nutzungsbedingungen / Terms of use:

CC BY-NC-ND 4.0

Dieses Dokument wird unter folgenden Bedingungen zur Verfügung gestellt: / This document is made available under these conditions:
CC-BY-NC-ND 4.0: Creative Commons: Namensnennung - Nicht kommerziell - Keine Bearbeitung
Weitere Informationen finden Sie unter: / For more information see:
https://creativecommons.org/licenses/by-nc-nd/4.0/deed.de

Geometric properties of integrable Kepler and Hooke billiards with conic section boundaries

Daniel Jaud [a,*], Lei Zhao [b]

[a] Gymnasium Holzkirchen, Jörg-Hube-Str. 4, Holzkirchen, Germany
[b] Institute of Mathematics, University of Augsburg, Universitätsstraße 2, Augsburg, Germany

1. Introduction

In 1868, Ludwig Boltzmann published an article [4] in which he thought established the ergodicity for a class of simple mechanical systems. The system he considered in particular contains the case of a point-like massive particle under the influence of a Keplerian $1/r-$potential and an ideally straight reflection wall. The orbit of the particle are arcs of Keplerian orbits. When hitting the reflection wall, it gets elastically reflected. As we see this defines a Kepler billiard system. In contrast to what Boltzmann asserted, it was recently shown in [8] that this system inhabits an additional integral of motion, is therefore integrable and non-ergodic. We next state this result:

Theorem 1 *(Gallavotti-Jauslin). Let F and F_i be the foci of a Kepler ellipse $\mathcal{K}_i$, where the center of force lies at F. Further consider a straight line l which the orbit of the Kepler ellipse $\mathcal{K}_i$ intersects at the point of reflection P. Then the focus F_{i+1} of the new reflected ellipse $\mathcal{K}_{i+1}$ lies on a common circle around the mirror image F_{mr} of F with respect to the line l with radius $|F_iF_{mr}|$.*

This additional first integral allowed G. Felder [7] to identify an associated elliptic curve for the compactification of the joint level set, an integration of the problem with a short computation on 3-periodic orbits. The computation on n-periodic orbits of the system has been continued by S. Gasiorek and M. Radnović [9]. In [18], this additional first integral is linked to the energy of a Kepler problem on the sphere.

* Corresponding author.
E-mail address: Daniel.Jaud.PhD@gmail.com (D. Jaud).

In a related situation, it has been shown [12] that the description of consecutive orbits in terms of the foci of a particle parabolic trajectory under the influence of a constant, uniform gravitational field, yields a fruitful analysis on the geometric properties of the system.

In dimension 2, the Kepler problem is dual to the Hooke problem via the complex square mapping [13,10]. Panov [15] observed that this extends to Kepler and Hooke billiards. An alternative way to establish the first integral of Gallavotti-Jauslin is presented in [17]. The Hooke billiards with a centered conic section domain is integrable, which follows from [11]. Their dynamics have been studied in e.g. [6] or [1].

Apart from the two distinct systems, it also appears in celestial mechanics [3] that combinations of the Hooke and Kepler system give rise to a reasonable approach to describe the dynamics of a massive object within and outside a region of a given mass distribution, in terms of refraction billiard systems they introduce. Their method covers the case of a Kepler billiard in an elliptic domain, and they showed that in the case the Kepler center is put at the center of the elliptic domain, then the Kepler billiard system is chaotic. In [2], Barutello and de Blasi explained that putting a Kepler center in a generic position inside an ellipse always results in a chaotic billiard system.

The main purpose of this work is to consider some geometric properties of the second foci in other integrable Hooke and Kepler billiards reflected at a conic section in the plane.

The structure of this paper is as follows: In Section 2 we introduce necessary concepts and general settings that will be used throughout this paper. In Section 3, we discuss the geometric interpretation of the additional first integral of the Kepler billiards from [17], and describe the construction procedure of consecutive Kepler orbits in terms of consecutive (second) foci, which in general can be applied to Kepler billiards with other reflection walls. In addition, we will derive some geometric properties of the system such as the focal reflection property as well as the envelope curves of the directrices of consecutive Kepler orbits (note that instead of the term "envelope" one also could call it a caustic to the orbit). In Section 4 we apply the conformal duality between the Hooke and Kepler system to carry the discussions to the Hooke billiards.

In particular, we show that in the corresponding Hooke billiards, consecutive foci of the Hooke orbits lie on certain Cassini ovals. We have thus identified a simple geometric property for which the Kepler side is simpler than the Hooke counterpart.

2. Setup

We consider the motion in a plane of a massive, point-like particle under the influence of either a Kepler or Hooke potential from the origin of the coordinate system. The Hamiltonians of the two systems are given respectively by

$$H_K = \frac{p_x^2 + p_y^2}{2m} + \frac{\alpha}{\sqrt{x^2 + y^2}},$$

and

$$H_H = \frac{p_x^2 + p_y^2}{2m} + \frac{k}{2} \cdot \left(x^2 + y^2\right).$$

Depending on the sign of the coupling constants α and k and the energy, the orbits of the particle are either ellipses or hyperbolic arcs, or parabolas in the case of zero-energy in the Kepler case. We shall mainly focus on elliptic orbits in this study. The extensions to other types of orbits are straightforward. For the elliptical orbits we will also use the term flight ellipse to indicate the ellipse containing the orbit arc outside the boundary. We will describe the corresponding flight ellipses in terms of their foci and semi-major axis a. The particle is further assumed to reflect ideally according to the classical law of reflection along a conic section boundary $\mathcal{B}$, also called mirror, and otherwise propagates under the influence of the potential. We consider them to be oriented clock-wise if they are not degenerated to a line segment to have a well-defined billiard dynamics. We will refer to these dynamical systems as Kepler billiards and Hooke billiards respectively.

We consider the Kepler billiard with the mirror boundary given by the *focused* conic section

$$\mathcal{B}_K : \frac{(x - \mathbf{c_K})^2}{\mathbf{a_K^2}} + \frac{y^2}{\mathbf{a_K^2} - \mathbf{c_K^2}} = 1.$$

In the non-degenerate cases, the foci of such a conic lie at $F := (0, 0)$ and $F' := (2\mathbf{c_K}, \mathbf{0})$. The semimajor axis of $\mathcal{B}_K$ is $\mathbf{a_K}$. The linear eccentricity $\mathbf{c_K}$, which is the product of $\mathbf{a_K}$ with the eccentricity e_K, equals to the half distance between the two foci: $2\mathbf{c_K} = |\mathbf{FF'}|$.

In order to distinguish the boundary parameters from the dynamical flight orbits we use bold letters for the boundaries parameters. The label **K** corresponds to the system with the Kepler potential whereas the label **H** associated with the Hooke potential will be used later on.

For $\mathbf{c_K} < \mathbf{a_K}$ we obtain ellipses as a boundary, for $\mathbf{c_K} > \mathbf{a_K}$ hyperbolic arcs. Our main focus will lie on those two boundary configurations. On the other hand, many of our analysis extends to circular or parabolic boundaries by taking necessary limits.

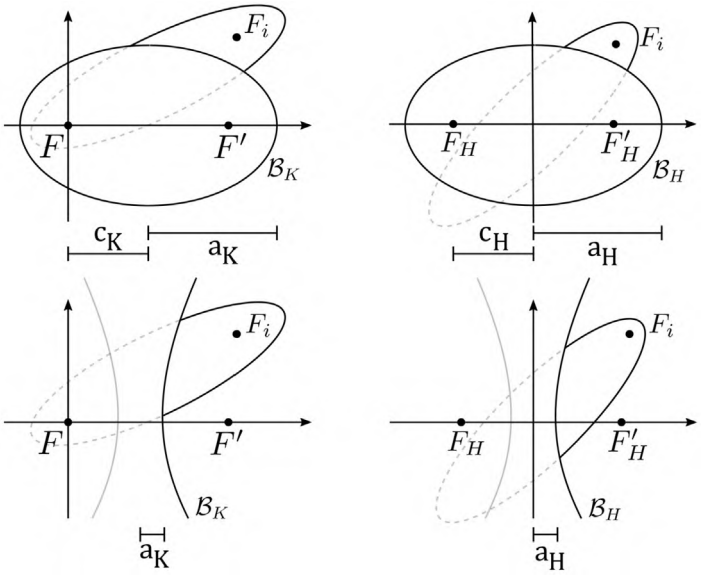


Fig. 1. *Left:* Representations of the considered cases for the Kepler system. *Right:* Representation of the considered cases for the Hooke system.

For the Hooke system, we consider the boundary given by a *centered* conic section

$$\mathcal{B}_H : \frac{x^2}{\mathbf{a_H}^2} + \frac{y^2}{\mathbf{a_H}^2 - \mathbf{c_H}^2} = 1,$$

where again depending on the value of the semi-major axis $\mathbf{a_H}$ with respect to the linear eccentricity $\mathbf{c_H}$ we obtain an elliptic or hyperbolic boundary.

In contrast to the Kepler system the foci $F_H := (-\mathbf{c_H}, 0)$ and $F'_H := (\mathbf{c_H}, 0)$ of the Hooke boundary $\mathcal{B}_H$ lie symmetrically around the origin, at which the center of the force locates.

The motion of the associated ellipses for the Kepler or Hooke system can in principle lie on either side of the corresponding boundaries, with closely-related dynamics. We mainly focus on the region not containing the origin. Some representative cases are displayed in Fig. 1.

For the cases where the orbits lie in the domain containing the origin, the Hooke center is regular but the Kepler center is singular. Nevertheless, it is classically known that collisions with the Kepler center can be regularized by exactly the Hooke-Kepler correspondence which we shall use. With the regularization, the orbits continue backward after bouncing back at the Kepler center. This consideration allows us to establish most of our analysis in these cases as well.

In all systems, the consecutive *flight ellipses* are characterized in terms of the energy and their consecutive foci. In the Kepler case, with the origin as a focus, the flight ellipses are completely determined by the positions of the *second foci* F_i and the conserved energy E. In the Hooke system, the pair of foci $\{F_i, -F_i\}$ as well as the energy E determine the form of the flight ellipse. We denote the consecutive orbits in the Kepler case by $\mathcal{K}_i$ and for the Hooke system by $\mathcal{H}_i$.

These mechanical billiard systems are known to be integrable in the sense that there exists an additional first integral independent of the energy [11,6,15,17,16]. In the next section we discuss this additional first integral and its geometrical implications in the Kepler case.

3. Kepler billiards

3.1. First integrals and envelopes

In this section we derive the first integral in addition to the total energy for the Kepler billiard we set up. We first present a geometrical proof. Then we show that this agrees with the geometrical interpretation of the first integral established in [17].

As already mentioned in Section 2 the associated consecutive Kepler flight ellipses, denoted by $\mathcal{K}_i$ with $i \in \mathbb{N}$, can be described by the position of the second focus F_i and the total energy $E < 0$ of the particle. Since we have $E \sim 1/a$ from the study of Kepler problem, geometrically, the conservation of the total energy easily translates into the conservation of the semi-major axis a for all $\mathcal{K}_i$. We will denote the second focus of $\mathcal{K}_i$ by $F_i = (F_{x,i}, F_{y,i})$.

Lemma 1. *Let P be the point of reflection along the boundary $\mathcal{B}_K$ of a Kepler ellipse $\mathcal{K}_i$ with foci F and F_i. Then the second focus F_{i+1} of the reflected ellipse $\mathcal{K}_{i+1}$ satisfies $|PF_i| = |PF_{i+1}|$.*

This is a direct consequence of the definition for an ellipse and the preservation of the semi-major axis a of the flight ellipses.

Having introduced all relevant definitions for the Kepler billiard, we now state the first theorem describing a common curve on which the consecutive foci F_i lie on. In [12] these curves were coined *foci curves*. Here we will adopt this notion.

Theorem 2 *(The foci circle in the Kepler case). Consider the Kepler billiard with Kepler center F with orbits outside a conic section boundary $\mathcal{B}_K$ with foci F and F'. Let $\mathcal{K}_1$ be a Kepler ellipse (hyperbola) with foci F and F_1. Then all the second foci F_i of consecutive flight Kepler ellipses (hyperbolas) $\mathcal{K}_i$ lie on a common circle around the second focus F' of $\mathcal{B}_K$ with radius $R = |F'F_i| = const$. In particular, R is a first integral in addition to the energy of this system.*

The theorem gives a geometric interpretation of the first integral derived in [17]. Note that in the case of a circular boundary, the two foci F and F' coincide. Also, the parabolic boundary may be viewed as the limiting case of a hyperbolic boundary where the distance between the foci F and F' is very large. In this case, one can effectively produce a particle bouncing inside a parabolic mirror with constant gravitational force. For this limiting case, the theorem reproduces the same result obtained in [12]. Alternatively, the limit $\mathbf{a_K} \to 0$ reproduces the theorem of Gallavotti-Jauslin 1 for the reflection along a straight line. For the proof of this Theorem 2 we only consider the elliptic boundary case. The result for the hyperbolic boundary then follows by the same arguments. The equivalent results for the circular and parabolic boundary follow by the aforementioned limits.

Proof. Consider Fig. 2 *Bottom*. Without loss of generality let the initial flight ellipse with second F_1 intersect $\mathcal{B}_K$ at the point of reflection $P \in \mathcal{B}_K$.

We apply Theorem 1 with respect to the tangent line of $\mathcal{B}_K$ at P. So let F_P be the mirror point of F with respect to the tangent line at P. Since $|FP| = |F_P P|$ and, due to the optic property of the ellipse, we see that F_P lies on the straight line through P and F'. Applying Lemma 1 and Theorem 1 we obtain F_2 as the intersection point of the circle centered at F_P with radius $|F_P F_1|$ and the other circle centered at P with radius $|PF_1|$.

Thus F_2 is the mirror point of F_1 with respect to the line $\overline{F'P}$, and thus $|F_1F'| = |F_2F'|$. Since the same construction holds true for all consecutive flight ellipses, it follows that $|F'F_i| = |F'F_1| = R = const.\ \forall i \in \mathbb{N}$.

Note that the construction procedure by intersecting two circles to obtain consecutive foci also works for other general boundaries not necessarily being conic sections. Thus, in general, consecutive foci F_i can be obtained numerically via a simple algorithm.

Next we provide another proof of the above theorem which illustrates the geometrical meaning of the Gallavotti-Jauslin first integral D as discussed in [17]. This directly covers the hyberbolic boundary case and the cases of combinations of confocal conic sections as well.

Proof. Let L be the angular momentum, $A = (A_1, A_2)$ the Laplace-Runge-Lenz vector, m the mass of the particle, E its energy and $\alpha < 0$ the coupling constant of the Kepler potential which we assume to be attractive. It has been shown [Lem 2, [17]] that for the elliptic boundary the quantity

$$D = L^2 - 2\mathbf{c_K} A_1$$

is a conserved quantity. As in [7], (at least) in the case of $\alpha < 0$, we may use the classical relationship

$$A_1^2 + A_2^2 = m^2\alpha^2 + 2mEL^2$$

to write D as

$$D = \frac{A_1^2 + A_2^2}{2mE} - 2\mathbf{c_K} A_1 - \frac{m\alpha^2}{2E}.$$

The normalized vector $\frac{1}{mE}\vec{A}$ is the vector connecting the origin to the second focus of the elliptic orbit, i.e. it is equal to $\vec{F}_i$.

By completing the square in the above equation we have

$$(\frac{A_1}{mE} - 2\mathbf{c_K})^2 + (-\frac{A_2}{mE})^2 = 4\mathbf{c_K}^2 + \frac{\alpha^2}{E^2} + \frac{2D}{mE}.$$

This means that the second focus F_i of the reflected elliptic orbits lies on a circle centered at the second focus $(2\mathbf{c_K}, 0)$ of the elliptic reflection wall, with radius given by

$$R = \sqrt{4\mathbf{c_K}^2 + \frac{\alpha^2}{E^2} + \frac{2D}{mE}}.$$

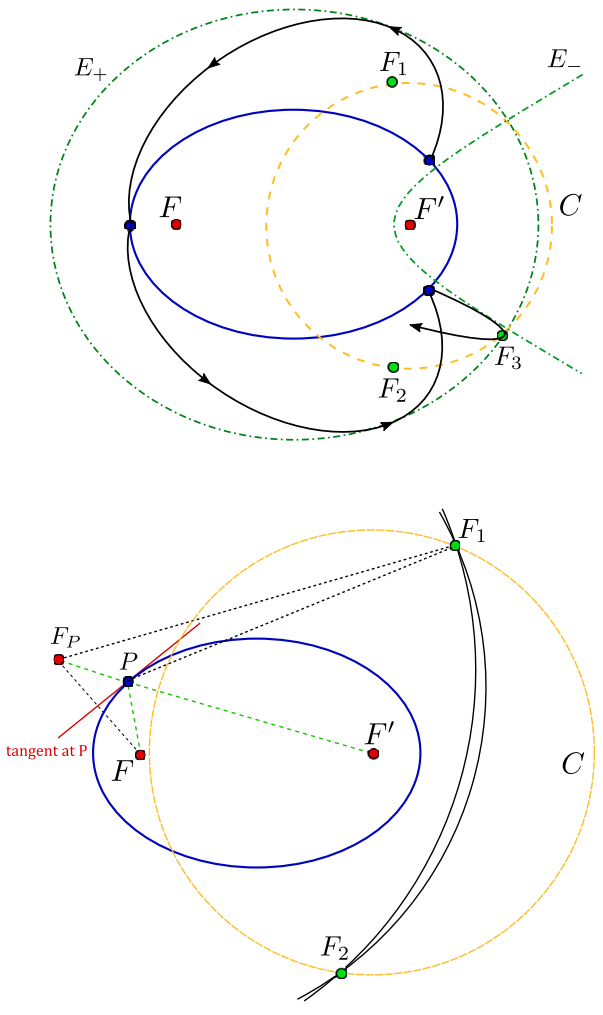


Fig. 2. *Top:* Consecutive flight ellipses with reflection along elliptic boundary and envelope curves $E_\pm$ (dash-dotted). *Bottom:* Geometric construction of consecutive foci F_i lying upon the same circle C (dashed) around F'.

Changing signs of α and E in the above argument extends the result to hyperbolic attractive and repulsive Kepler arcs as well.

As a last analysis for this section we derive the equations of the envelope curves $E_\pm$ of the flight ellipses. In our setting, these envelope curves are the analogues to the caustics of standard billiards in the plane.

Corollary 1. *The flight ellipses $\mathcal{K}_i$ are confined by the boundary itself and two envelope curves $E_\pm$ given by confocal conics with the same foci F and F' as the boundary $\mathcal{B}_K$. The equations for the envelopes read*

$$E_\pm : \frac{(x-\mathbf{c_K})^2}{\left(a \pm \frac{R}{2}\right)^2} + \frac{y^2}{\left(a \pm \frac{R}{2}\right)^2 - \mathbf{c_K^2}} = 1.$$

Here as before R is the radius of the foci curve, $\mathbf{c_K}$ is the linear eccentricity of the conic section boundary and a is the conserved semi-major axis of the Kepler orbit $\mathcal{K}_i$.

Proof. The proof follows by a direct computation of the envelope curve. For this each Kepler orbit $\mathcal{K}_i$ can be seen as the set of points $(x, y) \in \mathbb{R}^2$ satisfying

$$\mathcal{K}_i : K(x, y, \alpha_i) = 16a^2(x^2+y^2) - (F_{x,i}^2 + F_{y,i}^2 - 4a^2 - 2xF_{x,i} - 2yF_{y,i})^2 = 0,$$

with $F_{x,i} = 2\mathbf{c_K} + R\cos(\alpha_i)$ and $F_{y,i} = R\sin(\alpha_i)$, where α_i represents the angle labelling the position of the second focus F_i. The corresponding envelope curves $E_\pm$ then follows by solving the two equations

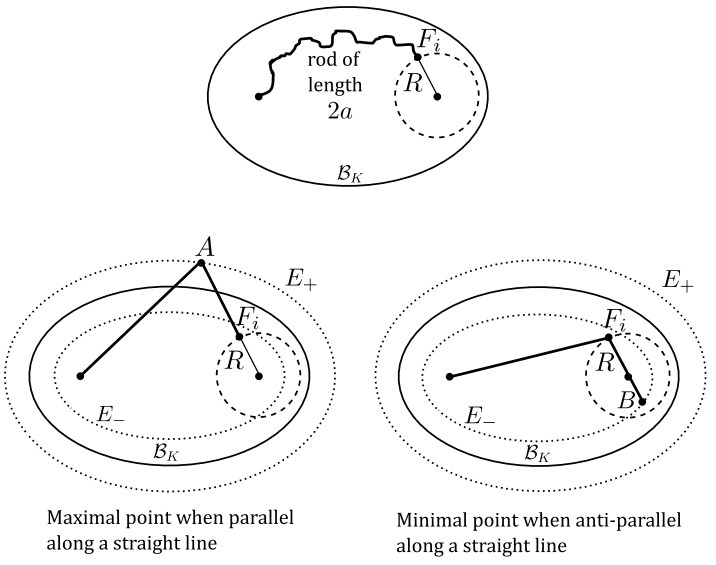


Fig. 3. Representative "string construction" for the two envelope curves corresponding to two confocal ellipses.

$$K(x, y, \alpha_i) = 0,$$
$$\partial_{\alpha_i} K(x, y, \alpha_i) = 0.$$

For a graphical representation of the confocal envelope curves in the elliptic boundary scenario see e.g. Fig. 2 *Top*.

Geometrically, if one considers the explicit form of $E_\pm$, one can interpret these curves with the "string construction" of ellipses/hyperbolas with foci $F = (0, 0)$ and $F' = (2\mathbf{c_K}, 0)$ and string of length $|2a \pm R|$ respectively. Here the set of extremal points A on $\mathcal{K}_i$ forming E_+ are those points where the string is aligned with the direction of $\overline{F'F_i}$. Similarly, the set of points B forming E_- are points on $\mathcal{K}_i$ where the string is aligned in the opposite direction of $\overline{F'F_i}$ (compare Fig. 3). In particular, this shows that each Kepler orbit $\mathcal{K}_i$ contains exactly two extremal points (A, B) with respect to the string constructions, with $A \in E_+$ and $B \in E_-$.

Depending on the choice of a, R and $\mathbf{c_K}$, the envelope curves correspond to confocal ellipses or hyperbolic arcs. The result is similar to the envelope curves obtained for the straight line system as discussed in [9]. Note that for the hyperbolic boundary case in the limit $\mathbf{c_K} \to \infty$ the system is equivalent to a particle bouncing inside a parabolic mirror with constant gravitational force as discussed e.g. in [12].

3.2. Focal reflection property

In this section we consider the billiard dynamics of a Kepler ellipse $\mathcal{K}_i$, whose orbit is passing through the second focus F' of the boundary $\mathcal{B}_K$. This is the case, when the semi-major axis a, the linear eccentricity $\mathbf{c_K}$ of the boundary and the radius R of the foci circle C satisfy a special condition stated in the Theorem 3 below.

We first discuss several lemmas.

Lemma 2. *Any flight ellipse $\mathcal{K}_i$ intersects $\mathcal{B}_K$ at most at two points.*

We postpone the proof to Section 4.

Lemma 3. *Let a Kepler flight ellipse $\mathcal{K}_i$ be degenerate to a line segment and contained in the x-axis, with the second focus $F_i = (F_{x,i}, 0)$ and major axis length $2a = |FF_i| = |F_{x,i}|$. Then either*

$$F_{x,i} < \mathbf{c_K} - \mathbf{a_K}$$

or

$$F_{x,i} > \mathbf{a_K} + \mathbf{c_K}.$$

The consequent motion of the particle is periodic, with reflections either at the pericenter or the apocenter of the elliptic boundary $\mathcal{B}_K$.

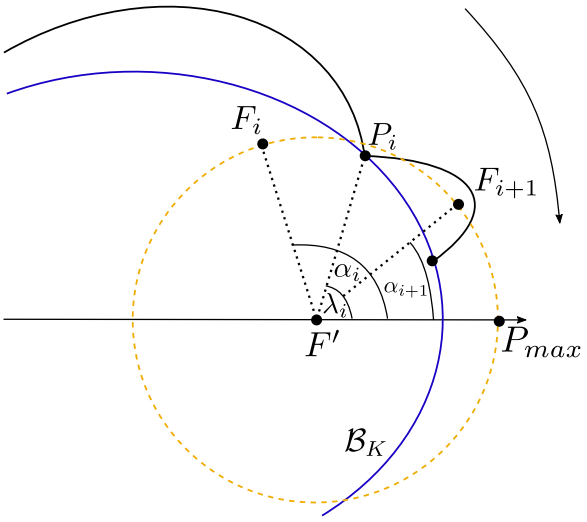


Fig. 4. Zoomed-in version of the graphical representation for the asymptotic behaviour of Kepler ellipses "passing" theoretically through F'.

Proof. The two restrictions on $F_{x,i}$ follow from the consideration that part of the Kepler orbit lie outside of the elliptic boundary $\mathcal{B}_K$ along the $x-$axis.

With this Lemma we can now formulate our main theorem of this section, which states the focal reflection property in our setting. This property is well-known for standard billiards in the plane. Felder's analysis showed a similar phenomenon exists for the line boundary case. The following theorem, stated for the case of a focused elliptic boundary, provides a generalization. As we will see, only one of the two degenerate orbits exists with the particular parameter setting in the following theorem, which plays the role of the nodal point as in [7].

We call a Kepler flight ellipse *admissible* if E_+ lies outside $\mathcal{B}_K$, and if

$$R > 0,\ 2a = R + 2\mathbf{c_K}$$

holds, which implies in particular that E_- is degenerated into the line segment FF' in $\mathcal{B}_K$. Clearly, if a Kepler flight ellipse is admissible, then so is any other Kepler flight ellipse on its billiard orbit. All of them intersect $\mathcal{B}_K$ at two points, which permit the definition of a complete forward billiard orbit starting from any of them. The condition $R > 0$ is included to permit non-stationary billiard orbits to exist.

Theorem 3 *(Focal reflection property). All admissible flight Kepler ellipses pass through F'. Furthermore, if an admissible flight Kepler ellipse does not degenerate into a line segment lying on the designated $x-$axis through F and F', then along the billiard orbit, the flight Kepler ellipses asymptotically converge to the degenerate line segment between F and the point $P_{max} = (0, R + 2\mathbf{c_K})$.*

Proof. A flight Kepler ellipse $\mathcal{K}_i$ is admissible if in particular $2a = R + 2\mathbf{c_K}$ holds, where $R = |F'F_i|$. This condition is equivalent to

$$2a = |FF'| + |F'F_i|.$$

Thus $\mathcal{K}_i$ passes through F'.

We now prove the second statement of the theorem. We take the FF'-axis as the reference axis equal to the $x-$axis. The point P_{max} lies on this axis. We label the position of F_i by the angle $\alpha_i = \angle P_{max}F'F_i$. Similarly we label the reflection point P_i of $\mathcal{K}_i$ (assumed clock-wise oriented when non-degenerate) with $\mathcal{B}_K$ by the angle $\lambda_i = \angle P_{max}F'P_i$ (see Fig. 4).

We assume that $0 < \alpha_i < 2\pi$. We first observe that always $0 < \lambda_i < \alpha_i < \lambda_{i+1}$. This follows from the string construction used in the proof of Corollary 1. Indeed it follows by this construction that the two intersection points of $\mathcal{K}_i$ with $\mathcal{B}_K$ lie on the different sides of the line $F'F_i$ which realizes the two extremal points as depicted in Fig. 3.

Consequently the sequence $\{\alpha_i\}_{i=1,2,3\ldots}$ is strictly decreasing. Moreover, we have the relationship

$$\alpha_{i+1} = \alpha_i - 2(\alpha_i - \lambda_i),$$

which follows from the mirror construction of F_{i+1} from F_i as described in Lemma 1.

We now show $\lim_{i\to\infty}\alpha_i = 0$. By monotonicity there exists $0 \le \alpha^* < 2\pi$ such that $\lim_{i\to\infty}\alpha_i = \alpha^*$. Consider the limit of the flight ellipses, which by construction has only one intersection with $\mathcal{B}_K$ and is therefore a degenerate Kepler ellipse, or

a line segment, which is fixed by the billiard mapping, so it has to lie in the major axis of $\mathcal{B}_K$, thus $\alpha^* \in \{0, \pi\}$. For the case $\alpha^* = \pi$ we see that the degenerate flight ellipse does not pass through F' and cannot be obtained as a limit of a sequence of Keplerian flight ellipses who do so. Thus the only possibility is $\alpha^* = 0$ and the limiting Keplerian ellipse is given by the degenerate line segment FP_{max}.

We remark that a similar statement holds for a focused hyperbolic branch boundary not enclosing the Kepler center. Moreover, this focal reflection property holds true for a parabolic mirror, since this can be seen as the limiting case of the elliptic/hyperbolic boundary. In the limiting case $\mathbf{c_K} \to \infty$, one obtains the motion in a focused parabolic mirror under the influence of a constant gravitational force as studied e.g. in [14,12]. In the centered circle boundary case, orbits are straight lines and the system is highly symmetric. The focal reflection property breaks down.

Note that Theorem 3 is a generalization of the equivalent result obtained in the Boltzmann system as discussed by [9].

3.3. The family of directrices in the Kepler billiard system

To conic sections with a preferred focus, we can associate a directrix d. The family of Kepler ellipses $\mathcal{K}_i$ with the preferred focus at the origin gives rise to a family of directrices d_K.

In this section, we investigate the geometry of the directrices in our integrable Kepler billiards. The result can be extended to various other cases, such as orbits of the attractive/repulsive Kepler problem inside $\mathcal{B}_K$.

Lemma 4. *Let the coordinate of the second Kepler focus be*

$$F_i = (F_x, F_y) = (2\mathbf{c_K} + R\cos(\alpha_i), R\sin(\alpha_i)).$$

Then the directrix d_K of an Kepler elliptic orbit $\mathcal{K}_i$ with the second focus F_i associated to the angle α_i is given by:

$$d_K := x \cdot F_x + y \cdot F_y + 2a^2 - \frac{1}{2} \cdot (F_x^2 + F_y^2) = 0. \tag{1}$$

Proof. Let $\mathcal{K}_i$ be a Kepler flight ellipse with semi-major axis a, with the preferred focus F at the origin and F_i as defined above. The distance of the closest point $P \in d_K$ from the origin is given by $|OP| = \frac{a}{e} - ae$, where e is the excentricity, related to the foci distance by $ae = \frac{1}{2}|\vec{F}_i|$. Thus the point $P \in d_K$ has the expression

$$\vec{P} = -\frac{\vec{F}_i}{|\vec{F}_i|} \cdot \left(\frac{a}{e} - ae\right) = -\frac{\vec{F}_i}{|\vec{F}_i|^2} \cdot \left(2a^2 - \frac{1}{2}|\vec{F}_i|^2\right).$$

The directrix has to run perpendicular to $\vec{F}_i$ through P, i.e. it has to take the form

$$d_K : \vec{x} = \begin{pmatrix} x \\ y \end{pmatrix} = \vec{P} + \lambda \begin{pmatrix} -F_y \\ F_x \end{pmatrix}, \quad \lambda \in \mathbb{R},$$

with the point P on it. Plugging in the expression of P we determine λ and consequently the expression for d_K.

Along a billiard orbit, the family of directrices has an envelope. By an *envelope curve* we mean a curve which contains the envelope of the family of directrices along a billiard orbit with the first integrals being fixed. We shall obtain such a curve from the foci curve. Depending on the relation between $2\mathbf{c_K}$ and R, this curve is given by different conic sections.

Theorem 4. *If $2\mathbf{c_K} \neq R$, then the envelope of the family of directrices is contained in either an ellipse or a hyperbola. The equations for these two conic sections are*

$$\frac{4(R^2 - 2\mathbf{c_K})^2 \cdot \left(x + \mathbf{c_K} \cdot \frac{4\mathbf{c_K}^2 - R^2 - 4a^2}{R^2 - 4\mathbf{c_K}^2}\right)^2}{R^2 \cdot (4a^2 + 4\mathbf{c_K}^2 - R^2)^2} + \frac{4(R^2 - 4\mathbf{c_K}^2) \cdot y^2}{(4a^2 + 4\mathbf{c_K}^2 - R^2)^2} = 1.$$

For $2\mathbf{c_K} = R$, i.e. when the foci circle C is passing through F, the envelope curve for the family of directrices is the parabolic arc with the equation

$$x = \frac{\mathbf{c_K}}{2a^2} \cdot y^2 - \frac{a^2}{2\mathbf{c_K}} + 2\mathbf{c_K}.$$

For all cases one focus of these conic sections lies at $F'(2\mathbf{c_K}, 0)$, i.e. the second focus of $\mathcal{B}_K$. The second focus for case $2\mathbf{c_K} \neq R$ lies at $\left(-\frac{8a^2\mathbf{c_K}}{4\mathbf{c_K}^2 - R^2}, 0\right)$.

Proof. The envelope curve for the family of directrices we look for is determined by

$$d_K(x, y, \alpha_i) = 0, \quad (I)$$
$$\partial_{\alpha_i} d_K(x, y, \alpha_i) = 0. \quad (II)$$

The explicit expression for d_K is given by

$$d_K = x(2\mathbf{c_K} + R\cos(\alpha_i)) + yR\sin(\alpha_i) + 2a^2 - 2\mathbf{c_K}^2 - \frac{R^2}{2} - 2\mathbf{c_K}R\cos(\alpha_i).$$

Condition (II) thus reads

$$-xR\sin(\alpha_i) + yR\cos(\alpha_i) + 2\mathbf{c_K}R\sin(\alpha_i) = 0,$$

and thus

$$\tan(\alpha_i) = \frac{\sin(\alpha_i)}{\cos(\alpha_i)} = \frac{y}{x - 2\mathbf{c_K}}.$$

We write

$$\sin(\alpha_i) = \frac{\epsilon\tan(\alpha_i)}{\sqrt{1+\tan^2(\alpha_i)}},$$
$$\cos(\alpha_i) = \frac{\epsilon}{\sqrt{1+\tan^2(\alpha_i)}},$$

where $\epsilon = \pm 1$ depending on the quadrant α_i lies in. Plugging in these expressions in (I) together with the result for $\tan(\alpha_i)$ obtained from (II) we obtain:

$$(I) \Leftrightarrow \frac{R\epsilon(x - 2\mathbf{c_K})}{\sqrt{1+\tan^2(\alpha_i)}} + \frac{R\epsilon y\tan(\alpha_i)}{\sqrt{1+\tan^2(\alpha_i)}} + 2x\mathbf{c_K} + \frac{1}{2}(4a^2 - 4\mathbf{c_K}^2 - R^2) = 0$$
$$\Leftrightarrow \frac{R\epsilon[(x-2\mathbf{c_K})^2 + y^2]}{\sqrt{(x-2\mathbf{c_K})^2 + y^2}} = -2x\mathbf{c_K} - \frac{1}{2}(4a^2 - 4\mathbf{c_K}^2 - R^2).$$

Squaring the above expression with $\epsilon^2 = 1$ we get

$$R^2[(x-2\mathbf{c_K})^2 + y^2] = [2x\mathbf{c_K} + \frac{1}{2}(4a^2 - 4\mathbf{c_K}^2 - R^2)]^2.$$

This is equivalent to

$$x^2(R^2 - 4\mathbf{c_K}^2) - 2\mathbf{c_K}x(4a^2 - 4\mathbf{c_K}^2 + R^2) + 4\mathbf{c_K}^2R^2 - \frac{1}{4}(4a^2 - 4\mathbf{c_K}^2 - R^2)^2 + R^2y^2 = 0,$$

from which the results in different cases follow. If $R^2 - 4\mathbf{c_K^2} = 0$, we obtain the parabolic envelope. Otherwise we obtain elliptic/hyperbolic envelopes described above.

Note that in the large $\mathbf{c_K}$ case, the hyperbolic boundary turns into a parabolic boundary. In this limit holds that $a \approx \mathbf{c_K} \gg R$ and one can perform a limit calculation for the envelope of directrices in this scenario to obtain

$$\frac{4\mathbf{c_K}^2x^2}{R^2(\mathbf{c_K}^2 + a^2)} - \frac{4\mathbf{c_K}^2y^2}{\mathbf{c_K}^2 + a^2} = 1.$$

This means that in the limit of a parabolic boundary the envelope of directrices is always given by a hyperbola.

4. Hooke billiards

4.1. The Hooke-Kepler correspondence

In two dimensions, the Kepler system is dual to the Hooke system. This and other dualities of power-law forces were first discovered by [13] and later on discussed in [10]. In particular, by identifying the plane with the complex plane, it is seen [10,13] that under the conformal mapping $z \mapsto z^2$, unparametrized trajectories of the Hooke system are mapped to unparametrized trajectories of the Kepler problem. In particular, the centered Hooke ellipses are mapped to focused Kepler ellipses. Moreover, it is not hard to check that both foci of the Hooke ellipse are mapped to the second focus F' of the Kepler ellipse: Say the Kepler ellipse is given by

$$|q| + |q - F'| = C_1$$

for a constant C_1. This means the pre-image satisfies

$$|z^2| + |z^2 - F'| = C_1. \tag{2}$$

Let $\sqrt{F'} \in \mathbb{C}$ be any square root of F'. We have

$$|z + \sqrt{F'}|^2 + |z - \sqrt{F'}|^2 = 2(|z|^2 + |F'|)$$

and

$$|z + \sqrt{F'}| \cdot |z - \sqrt{F'}| = |z^2 - F'|.$$

Thus, we obtain from (2) that

$$(|z + \sqrt{F'}| + |z - \sqrt{F'}|)^2 = C_2$$

for some constant C_2. Thus, the pre-image is an ellipse with foci $\pm\sqrt{F'}$.

Since the mapping is conformal, this correspondence extends to the corresponding billiard systems [15], [17]. The transformation also leads to many new classes of integrable mechanical billiards in systems similar to the Stark problem (Kepler problem with an external constant force field) [17].

Due to the linearity of the force in the Hooke system, as a rule, it is often easier to carry out investigations in the Hooke system than in the Kepler counterpart. Some questions concerning the Kepler problem become much apparent after being transformed into the Hooke problem. As an example, we first prove Lemma 2.

Proof. (of Lemma 2): The pre-images of both the flight ellipse and the boundary are centered ellipses. They intersect at most at four points, coming in pairs symmetric with respect to the center. Thus the image of the set of intersection points consists at most of two points.

As will be shown in the following, the computation of foci curve in the Kepler billiard here is one of the few examples, in which the calculations can be carried out in a much easier way in the Kepler billiard. The foci curve of the Hooke billiard is thus obtained in a simple fashion. It does not seem to be easy to be directly identified in the Hooke billiard though, as the curve is in general of degree 4.

4.2. The foci curve and the directrices

The integrability of Hooke billiards inside a centered conic section domain is well-known [11], [6]. Here we illustrate the geometric meaning of an additional first integral of these Hooke billiards.

We consider orbits of the attractive Hooke problem, which are centered ellipses $\mathcal{H}_i$ in the plane. As in the case of Kepler ellipses, it turns out useful to describe these ellipses at a given energy E in terms of their foci, which lie symmetrically with respect to the Hooke center that we put at the origin.

We denote one of the two foci by $F_i = (F_{x,i}, F_{y,i})$. The Hooke flight ellipse at given positive energy E with a focus at F_i is thus given by the equation:

$$\mathcal{H}_i : \left(x^2 + y^2 - \frac{2E}{k}\right)^2 = \left[(x - F_{x,i})^2 + (y - F_{y,i})^2\right] \cdot \left[(x + F_{x,i})^2 + (y + F_{y,i})^2\right].$$

Note that in contrast to the Kepler system, for which the semi-major axis a of the Kepler ellipse is conserved, the semi-major axis of the Hooke ellipse (denoted by a_H) does not relate in the same way to the total energy. It varies with the position of the focus according to

$$a_H = \sqrt{\frac{1}{2} \cdot (F_{x,i}^2 + F_{y,i}^2) + \frac{E}{k}}.$$

We can now state the first main theorem regarding the integrable Hooke billiard system.

Theorem 5 *(Hooke foci curve). Consider the Hooke billiard with a centered conic section $\mathcal{B}_H$ as boundary. Then the foci of a Hooke flight elliptic orbits lie on a foci curve given by a Cassini oval of the form*

$$[(x - \mathbf{c_H})^2 + y^2] \cdot [(x + \mathbf{c_H})^2 + y^2] = R_H^4,$$

where $\mathbf{c_H}$ is the linear eccentricity of $\mathcal{B}_H$ and R_H can be regarded as a generalised radius.

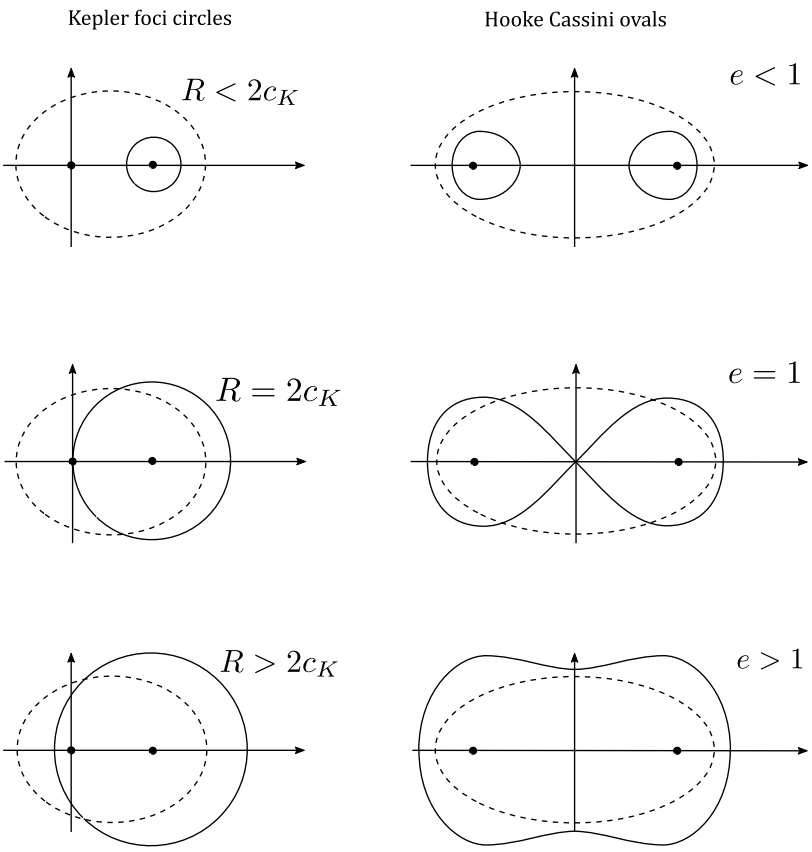


Fig. 5. Illustration of Cassini ovals (right) for different values of their corresponding eccentricity e and the related foci circles in the Kepler systems (left). The dashed lines correspond to the associated elliptic boundaries.

We denote the set of points $(x, y) \in \mathbb{R}^2$ lying on the Cassini curve by $\mathcal{C}(\mathbf{c_H}, R_H)$.

Proof. The foci curve in the Hooke system is the pre-image under the complex square mapping $\mathbb{C} \mapsto \mathbb{C}, \quad z \mapsto q = z^2$ of the foci curve of the associated Kepler system. The pre-image of the Kepler foci curve $|q - 2\mathbf{c_K}| = R$, which is a circle with radius R and centered at $(2\mathbf{c_K}, 0)$, is:

$$|z^2 - 2\mathbf{c_K}| = R$$

and thus

$$|z - \sqrt{2\mathbf{c_K}}| \cdot |z + \sqrt{2\mathbf{c_K}}| = R,$$

which describes a Cassini oval. In real coordinates $z = x + iy$ the equation reads

$$[(x - \mathbf{c_H})^2 + y^2] \cdot [(x + \mathbf{c_H})^2 + y^2] = R_H^4,$$

with $\mathbf{c_H} = \sqrt{2\mathbf{c_K}}$ and generalised radius $R_H = \sqrt{R}$.

The eccentricity of the Cassini oval is defined as

$$e := \frac{R_H}{\mathbf{c_H}}.$$

This parameter helps to distinguish the different shapes of the Cassini ovals.

Fig. 5 illustrates the obtained Cassini ovals for the different possibilities of the Cassini eccentricity e compared with the corresponding circles in the Kepler system and the elliptic boundary.

According to his son Jacques, Giovanni Domenico Cassini proposed that the Sun should move along one of these Cassini ovals around the earth, which occupies one of the Cassini foci [5].

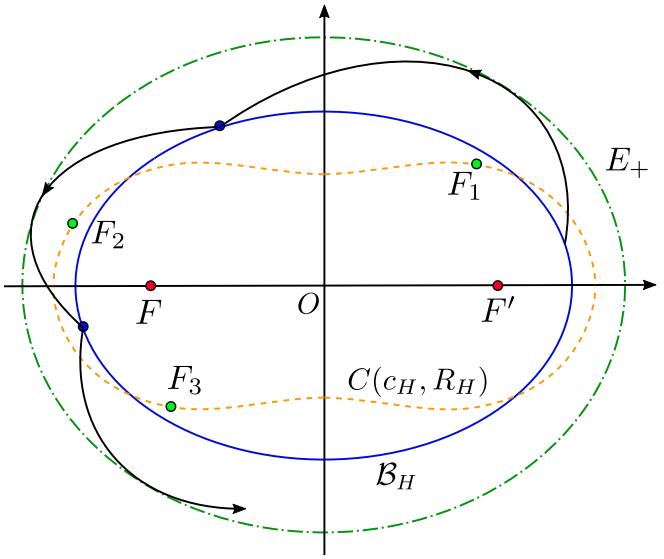


Fig. 6. Cassini foci curve $\mathcal{C}(\mathbf{c_H}, R_H)$ (dashed), associated flight ellipses and envelope E_+ (dash-dot) for $\mathbf{c_H} = 1$ and $R_H = \sqrt[4]{2}$. For these parameters the elliptic envelope E_- lies within $\mathcal{B}_H$ and therefore is not shown in the graphic.

The corresponding envelope curves associated to this integrable Hooke billiard system in the plane, as have been established in multi-dimensional case in [6] can as well be obtained in the planar case directly from the Kepler case as pre-images under the complex square mapping. We have

Corollary 2. *The envelope curves $E_{H\pm}$ in the integrable Hooke billiards with an elliptic boundary with foci F_H and $-F_H$ are given by confocal ellipses/hyperbolas with equations:*

$$E_{H\pm} = \frac{x^2}{\frac{1}{2}\cdot(\mathbf{c_H}^2 \pm R_H^2) + \frac{E}{k}} + \frac{y^2}{\frac{1}{2}\cdot(-\mathbf{c_H}^2 \pm R_H^2) + \frac{E}{k}} = 1,$$

where $\mathbf{c_H}$, R_H are the parameters of the Cassini foci curve $\mathcal{C}(\mathbf{c_H}, R_H)$ and E is the energy of the Hooke system.

In Fig. 6 one finds an illustration of the associated Hooke billiard with an elliptic boundary and envelope curve. As shown, the consecutive foci F_i for the Hooke flight orbits lie along the Cassini oval.

Note that in the limiting case where $R_H \gg \mathbf{c_H}$, i.e. $e \gg 1$, the foci curve resembles a circle of radius R_H centered at the origin.

4.3. The focal reflection property

Similar to the focal reflection property for the Kepler system we can state an equivalent property for the Hooke system.

We state the result in relation to the Kepler case. A Hooke flight ellipse is called admissible if its image is admissible in the corresponding Kepler system. In particular, geometrically an admissible Hooke ellipse passes through both foci of the elliptic boundary $\mathcal{B}_H$. This is the case if $\left(\mathbf{c_H} - \frac{2E}{k}\right)^2 = R_H^4$ is satisfied and the orbit is not degenerated to a straight line.

Theorem 6 *(Hooke focal reflection property). Let F_H and F'_H be the symmetric foci of the conic boundary $\mathcal{B}_H$ of the Hooke billiard. If one Hooke ellipse $\mathcal{H}_1$ passes through F_H and F'_H then all consecutive Hooke ellipses $\mathcal{H}_i$ pass through these points. Asymptotically, the Hooke ellipses tend to the axis of foci F_H and F'_H.*

Proof. This is a direct consequence of the Focal Reflection Property, Theorem 3 in the Kepler system. The Kepler conics passing through the second focus of the boundary are pulled back by $z \mapsto q = z^2$ to Hooke conics passing through both foci of the boundary. Without loss of generality, we may assume that the second focus of the Kepler boundary is on the positive real-axis. The foci of the Hooke boundary thus lie on the real axis, symmetric with respect to the origin. The foci of the flight ellipses thus converge to the pre-image of the point P_{max} which also lie on the real axis. In particular, they tend to the real axis.

4.4. The family of directrices in the Hooke system

For the Kepler system, we have derived the envelopes for the family of directrices and have seen that these correspond to (parts of) conic sections with a focus at the focus F' of the boundary $\mathcal{B}_K$.

For the Hooke system, we now carry out the same steps. Here we simply present a parametric expression for the envelope curves. These, in general, are algebraic curves of degree 4. Note that the directrices in the Hooke and Kepler system are not directly related by the complex square mapping, which does not preserve straight lines.

We aim to describe the foci of the Hooke flight ellipses $F_i \in \mathcal{C}(\mathbf{c_H}, R_H)$ in terms of $\mathbf{c_H}$ and R_H. In polar coordinates, we have $F_i = (r_\pm(\varphi), \varphi)$, where for the radius we have two different choices

$$r_\pm(\varphi) = \sqrt{\mathbf{c_H}^2 \cos(2\varphi) \pm \sqrt{\mathbf{c_H}^4 \cos^2(2\varphi) + R_H^4 - \mathbf{c_H}^4}},$$

corresponding to the 2 possible intersections of the ray with angle φ with $\mathcal{C}(\mathbf{c_H}, R_H)$.

The directrices of the Hooke ellipses are found by a direct computation, and are given by

$$d_H := x \cdot F_x + y \cdot F_y + \frac{1}{2} \cdot \left(F_x^2 + F_y^2\right) + \frac{E}{k} = 0,$$

with $F_x = r_\pm(\varphi) \cdot \cos(\varphi)$ and $F_y = r_\pm(\varphi) \cdot \sin(\varphi)$.

Theorem 7. *The envelope curve of the family of directrices of Hooke flight ellipses with* $\mathbf{c_H} > 0$ *are given in parametric form by*

$$x(\varphi) = -\left(\frac{E}{k \cdot (F_x^2 + F_y^2)} - \frac{1}{2}\right) \cdot \partial_\varphi F_y - F_x,$$
$$y(\varphi) = \left(\frac{E}{k \cdot (F_x^2 + F_y^2)} - \frac{1}{2}\right) \cdot \partial_\varphi F_x - F_y.$$

For $\mathbf{c_H} = 0$, i.e. *when* $\mathcal{B}_H$ *is a circle, the envelope of the directrices is given by the circle*

$$x^2 + y^2 = \frac{2E}{k}.$$

Proof. The envelope curve is determined by

$$d_H(x, y, \varphi) = 0, \quad (I)$$
$$\partial_\varphi d_H(x, y, \varphi) = 0. \quad (II)$$

We have

$$d_H(x, y, \varphi) = x \cdot F_x(\varphi) + y \cdot F_y(\varphi) + \frac{1}{2} \cdot \left(F_x(\varphi)^2 + F_y(\varphi)^2\right) + \frac{E}{k}.$$

Then by condition (II) it follows that

$$\partial_\varphi d_H = x \cdot \partial_\varphi F_x + y \cdot \partial_\varphi F_y + F_x \cdot \partial_\varphi F_x + F_y \cdot \partial_\varphi F_y = 0.$$

With $\vec{z} = (x, y)$, $\vec{F} = (F_x, F_y)^T$ this condition can be alternatively written as

$$[\vec{z} + \vec{F}(\varphi)] \cdot \partial_\varphi \vec{F}(\varphi) = 0.$$

The first solution to this equation is given by:

$$x(\varphi) = -\mu \cdot \partial_\varphi F_y - F_x,$$
$$y(\varphi) = \mu \cdot \partial_\varphi F_x - F_y,$$

where μ is a scaling parameter, which can then be uniquely determined by (I). Indeed, plugging these two expressions into (I), we have

$$\mu(F_y \cdot \partial_\varphi F_x - F_x \cdot \partial_\varphi F_y) - \frac{1}{2}(F_x^2 + F_y^2) + \frac{E}{k} = 0.$$

It is not hard to verify that

$$F_x \cdot \partial_\varphi F_y - F_y \cdot \partial_\varphi F_x = F_x^2 + F_y^2.$$

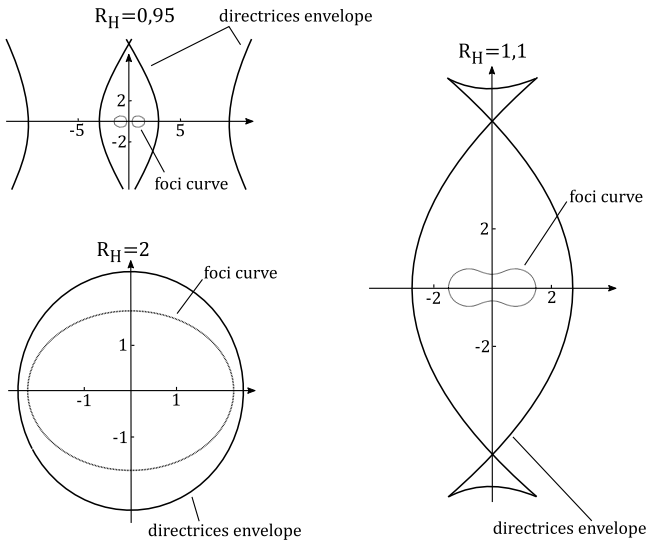


Fig. 7. Envelope curves for family of directrices for $R_H \in \{0.95, 1.1, 2\}$ at fixed $\mathbf{c_H} = 1$ and $E/k = 3$.

With these we obtain

$$\mu = \frac{E}{k \cdot (F_x^2 + F_y^2)} - \frac{1}{2}.$$

Plugging in this expression for the two coordinates x and y one obtains the result.

The second possible solution to the equation $[\vec{x} + \vec{F}(\varphi)] \cdot \partial_\varphi \vec{F}(\varphi) = 0$ is given by $\vec{z} = -\vec{F}(\varphi)$. We assume that a continuous part of the envelope curve is given by this second solution, as otherwise the first solution always holds. Inserting this in (I) yields

$$x^2 + y^2 = \frac{2E}{k},$$

which is a circle centered at the origin, with radius $\sqrt{2E/k}$. Since $\vec{z} = -\vec{F}$, the corresponding foci curve is given

$$F_x^2 + F_y^2 = \frac{2E}{k}.$$

This means that a continuous part of the foci curve is part of a centered circle. This is only possible if $\mathcal{C}(\mathbf{c_H}, R_H)$ is a circle, which is only possible if $\mathbf{c_H} = 0$, *i.e.* if $\mathcal{B}_H$ is a circle.

In Fig. 7 one finds various examples for the envelope of directrices for different parameters of R_H at fixed E/k and $\mathbf{c_H} > 0$.

Note that when R_H is large, the foci curve asymptotically resembles a circle centered at the origin with radius R_H. The corresponding envelope curve for the family of directrices also resembles a concentric circle with radius r given by

$$r = \frac{E}{k \cdot R_H} + \frac{1}{2} R_H.$$

Data availability

No data was used for the research described in the article.

Acknowledgements

Lei Zhao is supported by DFG ZH 605-1/2. We thank the anonymous reviewer to valuable suggestions for improvements.

References

[1] B. Barrera, J.P. Ruz-Cuen, J.C. Gutiérrez-Vega, Elliptic billiard with harmonic potential: classical description, Phys. Rev. E 108 (2023) 034205, https://doi.org/10.1103/PhysRevE.108.034205.

[2] V.L. Barutello, I.D. Blasi, A note on chaotic billiards with potentials, arXiv:2312.01312, 2023.

[3] V.L. Barutello, I.D. Blasi, S. Terracini, Chaotic dynamics in refraction galactic billiards, Nonlinearity 36 (2023) 4209–4246, https://doi.org/10.1088/1361-6544/acdec2.
[4] L. Boltzmann, Lösung eines mechanischen systems, Wien. Ber. 58 (1868) 1035–1044.
[5] J. Cassini, Elèments d'astronomie, A Paris, de l'Imprimerie royale. M. DCCXL, 1740.
[6] Y.N. Fedorov, An ellipsoidal billiard with a quadratic potential, Funct. Anal. Appl. 35 (2001) 199–208.
[7] G. Felder, Poncelet property and quasi-periodicity of the integrable Boltzmann system, Lett. Math. Phys. 111 (2021), https://doi.org/10.1007/s11005-020-01348-z.
[8] G. Gallavotti, I. Jauslin, A theorem on ellipses, an integrable system and a theorem of Boltzmann, arXiv:2008.01955, 2020.
[9] S. Gasiorek, M. Radnović, Periodic trajectories and topology of the integrable Boltzmann system, arXiv:2307.04991, 2023.
[10] E. Goursat, Les transformations isogonales en mécanique, C. R. Math. Acad. Sci. Paris 108 (1887) 446–450.
[11] C.G.J. Jacobi, Vorlesungen über Dynamik, Verlag von G. Reimer, 1866.
[12] D. Jaud, Gravitational billiards bouncing inside general domains - foci curves and confined domains, J. Geom. Phys. 194 (2023) 104998, https://doi.org/10.1016/j.geomphys.2023.104998, arXiv:2211.03788.
[13] C. Maclaurin, A treatise of fluxions, Ruddimans 2 (1742).
[14] S. Masalovich, A remarkable focusing property of a parabolic mirror for neutrons in the gravitational field: geometric proof, Nucl. Instrum. Methods Phys. Res., Sect. A, Accel. Spectrom. Detect. Assoc. Equip. 763 (2014) 517–520, https://doi.org/10.1016/j.nima.2014.07.004.
[15] A.A. Panov, Elliptical billiard table with Newtonian potential, Math. Notes 55 (1994) 334, https://doi.org/10.1007/BF02110789.
[16] A. Takeuchi, L. Zhao, Projective integrable mechanical billiards, Nonlinearity 37 (2023) 015011, https://doi.org/10.1088/1361-6544/ad0d6f.
[17] A. Takeuchi, L. Zhao, Conformal transformations and integrable mechanical billiards, Adv. Math. 436 (2024) 109411, https://doi.org/10.1016/j.aim.2023.109411.
[18] L. Zhao, Projective dynamics and an integrable Boltzmann billiard model, Commun. Contemp. Math. 24 (2022) 2150085, https://doi.org/10.1142/s0219199721500851.